The influence of low-symmetry distortions on electron transport through metal atom chains: when is a molecular wire really 'broken'?

Supporting information

Vihar Georgiev and John E. McGrady*

Department of Chemistry, Inorganic Chemistry Laboratory, University of Oxford, South Parks Road, Oxford, OX1 3QR, United Kingdom.

Complete reference 60

Baerends, E.J.; Autschbach, J.; Bérces, A.; Bickelhaupt, F. M.; Bo, C.; Boerrigter, P. M.; Cavallo, L.; Chong, D. P.; Deng, L.; Dickson, R. M.; Ellis, D. E.; van Faassen, M.; Fan, L.; Fischer, T. H.; Fonseca Guerra, C.; van Gisbergen, S. J. A.; Götz, A. W.; Groeneveld, J. A.; Gritsenko, O. V.; Grüning, M.; Harris, F. E.; van den Hoek, P.; Jacob, C. R.; Jacobsen, H.; Jensen, L.; van Kessel, G.; Kootstra, F.; Krykunov, M. V.; van Lenthe, E.; McCormack, D. A.; Michalak, A.; Neugebauer, J.; Nicu, V. P.; Osinga, V. P.; Patchkovskii, S.; Philipsen, P. H. T.; Post, D.; Pye, C. C.; Ravenek, W.; Rodriguez, J. I.; Ros, P.; Schipper, P. R. T.; Schreckenbach, G.; Snijders, J. G.; Solà, M.; Swart, M.; Swerhone, D.; te Velde, G.; Vernooijs, P.; Versluis, L.; Visscher, L.; Visser, O.; Wang, F.; Wesolowski, T. A.; van Wezenbeek, E. M.; Wiesenekker, G.; Wolff, S. K.; Woo, T. K.; Yakovlev, A. L.; Ziegler, T. ADF2008.01; SCM, Theoretical Chemistry, Vrije Universiteit: Amsterdam, The Netherlands, http://www.scm.com.

Influence of contact geometry.

We present here transmission spectra for two alternative contact geometries, the 'on-top/hollow' geometry that has been proposed as a model for break junction experiments (Figure S1) and a 'tilted' geometry where the molecule is aligned at an angle to the (111) surface of the gold electrode (Figure S2). Both figures should be compared to Figures 4a and 4c for the standard 'hollow/hollow' geometry. The transmission spectra (for both symmetric and unsymmetric Cr_3 chains) in the tilted geometry (Figure S2) are almost indistinguishable from those shown in Figures 3 and 4 for the 'hollow/hollow' geometry. In the 'on-top/hollow' geometry (Figure S1) the left hand ('on-top') sulphur is less strongly coupled to the electrode, and this reduces the size of the transmission peaks due to the π-symmetric orbitals (note particularly the reduction in spin-α (blue) intensity at E- E_f ~ -1.0 eV in the symmetric structure). The impact in the unsymmetric case is less obvious, simply because the π channels are less effective in any case due to the rehybridisation noted in the text. In terms of the computed conductance, however, the most significant point is that the σ^{nb} channel remains very close to the Fermi level, just as it is in the 'hollow/hollow' geometry. The transmission spectra for the tilted geometries are almost indistinguishable from those shown in Figures 3 and 4 for the 'hollow/hollow' geometry. The nature of the transport in these systems is clearly not strongly dependent on the precise details of the contact geometry.

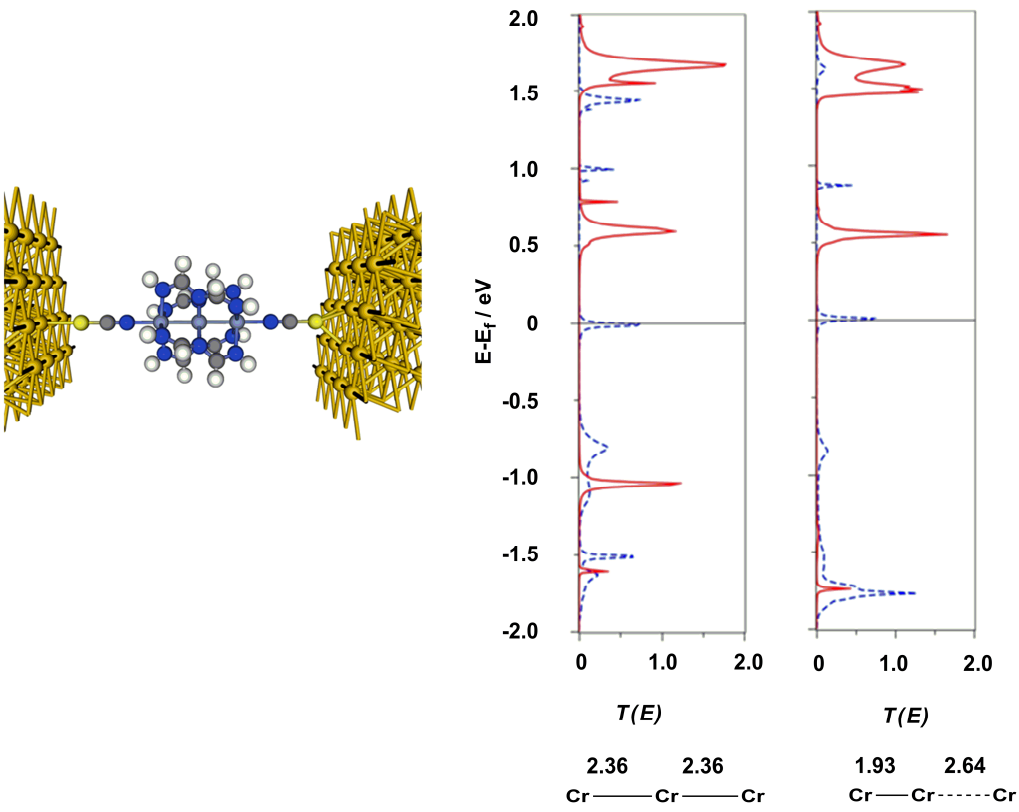

Figure S1 Transmission spectra for symmetric and highly unsymmetric Cr_3 chains in the ''on-top/hollow' geometry.

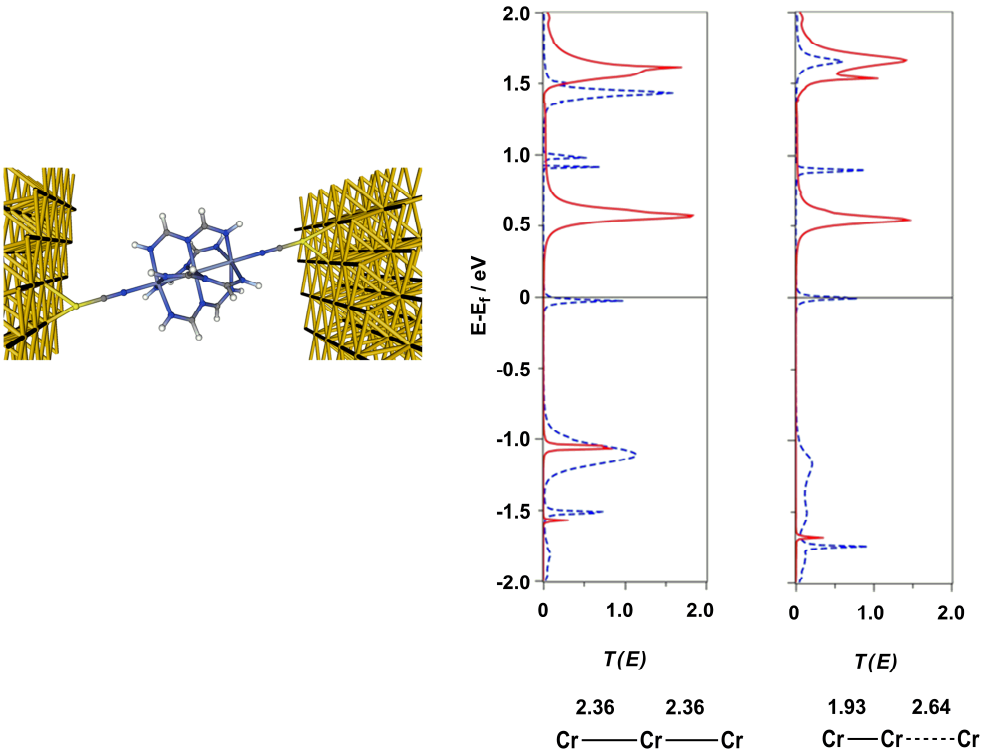

Figure S2 Transmission spectra for symmetric and highly unsymmetric Cr_3 chains in the 'tilted' geometry.

Influence of density functional

The calculations reported in the main text were performed using the LDA functional along with the Perdew-Zunger (PZ) correction for self-interaction error (SIE). The SIE is well known to influence the energies of occupied molecular orbitals, and Sanvito and co-workers have argued that corrections for this error (Self Interaction Corrections, SIC) are essential for the correct placement of the energy levels relative to E_f of an electrode such as gold (see for example ref 27). In exchange-coupled systems such as $Cr_3(L)_4(NCS)_2$ the SIC can cause significant changes in the spin density distribution, and hence in relative energies of the spin-α and spin-β manifolds of the isolated molecule. This is indeed the case here, and a parallel series of calculations performed using the gradient-corrected PBE functional gives substantially higher net spin densities on the Cr centres (Table S1). As a result the spin-α manifold is stabilised relative to its spin-β counterpart (this is the case both in the gas-phase and in the two-probe calculations), such that the σ^{nb} peak now lies ~0.7 eV *below* E_f in the symmetric system. The qualitative features associated with the structural deformation are precisely as noted for the LDA+PZ case in the main text: the distortion pushes the σ^{nb} level upwards towards the Fermi level. However, any minor shifts occur ~0.7 eV below the Fermi level, so now have minimal impact on the computed conductance. We note that the relative alignment of the levels for the GGA functional is inconsistent with both the higher measured conductance of Cr_3 vs Co_3 and also the facile oxidation of the former.

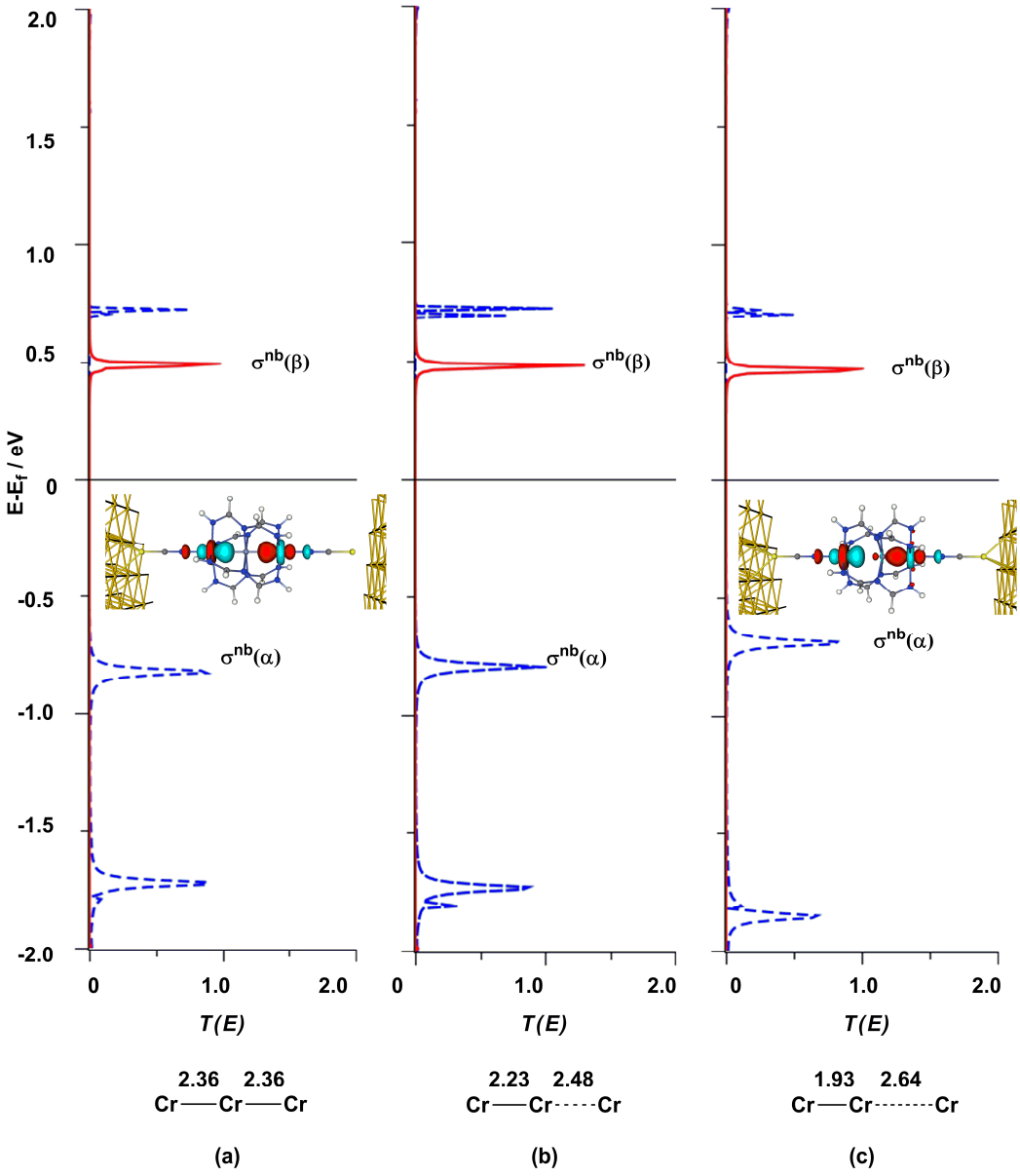

Figure S3 Transmission spectra for symmetric and highly unsymmetric Cr_3 chains using the PBE functional.

Table S1 Conductances and spin densities for the scattering regions obtained using the PBE functional.

Two-probe(ATK)

	Bond lengths / Å		Spin densities			Conductance ($G/\mu S$)		
	Cr_1-Cr_2	Cr_2-Cr_3	Cr_1	Cr_2	Cr_3	G_{tot}	G_α	G_β
s-$Cr_3(L)_4(NCS)_2$	2.36	2.36	3.85	-3.65	3.85	0.008	0.004	0.004
u-$Cr_3(L)_4(NCS)_2$ (0.25)	2.23(F)	2.48(F)	3.78	-3.58	3.90	0.014	0.007	0.007
u-$Cr_3(L)_4(NCS)_2$ (0.71)	1.93(F)	2.64(F)	3.45	-3.39	3.92	0.015	0.009	0.006

Total energies and Cartesian coordinates of stationary points (*s*-$Cr_3(L)_4(SCN)_2$, *u*-$Cr_3(L)_4(SCN)_2$ (0.25), *u*-$Cr_3(L)_4(SCN)_2$ (0.71).

Equilibrium structure *s*-$Cr_3(L)_4(NCS)_2$ (2.36 A)

E = -23.724818 au

Cr	0.000000	0.000000	-2.362422
Cr	0.000000	0.000000	0.000039
Cr	0.000000	0.000000	2.362660
N	-1.436592	-1.436203	-0.000161
N	1.436592	1.436203	-0.000161
N	1.436019	-1.436839	-0.000163
N	-1.436019	1.436839	-0.000163
N	-0.860419	-1.923940	-2.187945
N	0.860419	1.923940	-2.187945
N	1.923950	-0.860315	-2.187737
N	-1.923950	0.860315	-2.187737
N	-1.924006	-0.860612	2.187870
N	1.924006	0.860612	2.187870
N	0.860529	-1.924056	2.187941
N	-0.860529	1.924056	2.187941
N	0.000000	0.000000	4.451957
N	0.000000	0.000000	-4.451728
C	-1.447796	-2.340334	-1.023446
C	1.447796	2.340334	-1.023446
C	2.340247	-1.447934	-1.023340
C	-2.340247	1.447934	-1.023340
C	-2.340710	-1.447339	1.023088
C	2.340710	1.447339	1.023088
C	1.447105	-2.340903	1.023127
C	-1.447105	2.340903	1.023127
C	-1.918200	-3.666026	-0.912067
C	1.918200	3.666026	-0.912067
C	3.665929	-1.918357	-0.911920
C	-3.665929	1.918357	-0.911920
C	-3.666559	-1.917264	0.911411
C	3.666559	1.917264	0.911411
C	1.916918	-3.666798	0.911510
C	-1.916918	3.666798	0.911510
C	-0.761504	-2.784527	-3.223344
C	0.761504	2.784527	-3.223344
C	2.784621	-0.761230	-3.223053
C	-2.784621	0.761230	-3.223053
C	-2.784458	-0.762509	3.223465
C	2.784458	0.762509	3.223465
C	0.762513	-2.784412	3.223628
C	-0.762513	2.784412	3.223628
C	-1.233797	-4.082699	-3.176798
C	1.233797	4.082699	-3.176798
C	4.082802	-1.233499	-3.176475
C	-4.082802	1.233499	-3.176475

C	-4.082601	-1.234909	3.176826
C	4.082601	1.234909	3.176826
C	1.234784	-4.082601	3.177035
C	-1.234784	4.082601	3.177035
C	-1.814700	-4.528794	-1.984559
C	1.814700	4.528794	-1.984559
C	4.528800	-1.814618	-1.984306
C	-4.528800	1.814618	-1.984306
C	-4.529064	-1.814701	1.984180
C	4.529064	1.814701	1.984180
C	1.814385	-4.529215	1.984351
C	-1.814385	4.529215	1.984351
C	0.000000	0.000000	-5.649960
C	0.000000	0.000000	5.650182
H	-0.284654	-2.381283	-4.116316
H	0.284654	2.381283	-4.116316
H	2.381433	-0.284282	-4.116005
H	-2.381433	0.284282	-4.116005
H	-2.381153	-0.286291	4.116737
H	2.381153	0.286291	4.116737
H	0.286484	-2.380984	4.116945
H	-0.286484	2.380984	4.116945
H	-1.132892	-4.730005	-4.047061
H	1.132892	4.730005	-4.047061
H	4.730182	-1.132427	-4.046662
H	-4.730182	1.132427	-4.046662
H	-4.729705	-1.134829	4.047326
H	4.729705	1.134829	4.047326
H	1.134759	-4.729622	4.047603
H	-1.134759	4.729622	4.047603
H	-2.163977	-5.558503	-1.887937
H	2.163977	5.558503	-1.887937
H	5.558512	-2.163879	-1.887654
H	-5.558512	2.163879	-1.887654
H	-5.558786	-2.163927	1.887500
H	5.558786	2.163927	1.887500
H	2.163497	-5.558979	1.887710
H	-2.163497	5.558979	1.887710
H	-2.316124	-4.007630	0.042703
H	2.316124	4.007630	0.042703
H	4.007448	-2.316462	0.042805
H	-4.007448	2.316462	0.042805
H	-4.008448	-2.314164	-0.043706
H	4.008448	2.314164	-0.043706
H	2.313713	-4.008782	-0.043616
H	-2.313713	4.008782	-0.043616
S	0.000000	0.000000	-7.262074
S	0.000000	0.000000	7.262361

u-$Cr_3(L)_4(NCS)_2$ (0.25)

E = -23.724924 au

Cr	0.000000	0.000000	-2.418375

Cr	0.000000	0.000000	0.061625
Cr	0.000000	0.000000	2.291625
N	-1.445067	-1.423821	-0.016433
N	1.445067	1.423821	-0.016433
N	1.423691	-1.444988	-0.016375
N	-1.423691	1.444988	-0.016375
N	-0.852194	-1.922361	-2.202377
N	0.852194	1.922361	-2.202377
N	1.923014	-0.851179	-2.201615
N	-1.923014	0.851179	-2.201615
N	-1.930633	-0.854771	2.167732
N	1.930633	0.854771	2.167732
N	0.855412	-1.930542	2.167942
N	-0.855412	1.930542	2.167942
N	0.000000	0.000000	4.393735
N	0.000000	0.000000	-4.493496
C	-1.445317	-2.330500	-1.037441
C	1.445317	2.330500	-1.037441
C	2.331124	-1.443854	-1.036580
C	-2.331124	1.443854	-1.036580
C	-2.353443	-1.438061	1.003887
C	2.353443	1.438061	1.003887
C	1.439626	-2.352588	1.004342
C	-1.439626	2.352588	1.004342
C	-1.912183	-3.657431	-0.918565
C	1.912183	3.657431	-0.918565
C	3.658193	-1.910143	-0.917111
C	-3.658193	1.910143	-0.917111
C	-3.681816	-1.899251	0.892377
C	3.681816	1.899251	0.892377
C	1.905386	-3.679378	0.893398
C	-1.905386	3.679378	0.893398
C	-0.744070	-2.792778	-3.229382
C	0.744070	2.792778	-3.229382
C	2.793832	-0.742456	-3.228205
C	-2.793832	0.742456	-3.228205
C	-2.785984	-0.753253	3.206404
C	2.785984	0.753253	3.206404
C	0.755852	-2.785979	3.206690
C	-0.755852	2.785979	3.206690
C	-1.212905	-4.091692	-3.175105
C	1.212905	4.091692	-3.175105
C	4.093052	-1.210386	-3.173406
C	-4.093052	1.210386	-3.173406
C	-4.088214	-1.216130	3.160386
C	4.088214	1.216130	3.160386
C	1.224347	-4.086242	3.161802
C	-1.224347	4.086242	3.161802
C	-1.800160	-4.529213	-1.982557
C	1.800160	4.529213	-1.982557
C	4.530482	-1.797355	-1.980729
C	-4.530482	1.797355	-1.980729
C	-4.541519	-1.790454	1.967631
C	4.541519	1.790454	1.967631

C	1.800565	-4.538417	1.969528
C	-1.800565	4.538417	1.969528
C	0.000000	0.000000	-5.691900
C	0.000000	0.000000	5.591619
H	-0.264025	-2.396335	-4.123730
H	0.264025	2.396335	-4.123730
H	2.397699	-0.262201	-4.122597
H	-2.397699	0.262201	-4.122597
H	-2.376990	-0.280022	4.098285
H	2.376990	0.280022	4.098285
H	0.282807	-2.377614	4.098972
H	-0.282807	2.377614	4.098972
H	-1.105103	-4.745730	-4.039268
H	1.105103	4.745730	-4.039268
H	4.747498	-1.101788	-4.037171
H	-4.747498	1.101788	-4.037171
H	-4.733795	-1.111687	4.031371
H	4.733795	1.111687	4.031371
H	1.122579	-4.731449	4.033379
H	-1.122579	4.731449	4.033379
H	-2.147038	-5.558934	-1.878978
H	2.147038	5.558934	-1.878978
H	5.560380	-2.143610	-1.876850
H	-5.560380	2.143610	-1.876850
H	-5.574253	-2.130767	1.872836
H	5.574253	2.130767	1.872836
H	2.145078	-5.569850	1.875726
H	-2.145078	5.569850	1.875726
H	-2.314759	-3.992017	0.036596
H	2.314759	3.992017	0.036596
H	3.992653	-2.312029	0.038448
H	-3.992653	2.312029	0.038448
H	-4.027970	-2.292232	-0.062786
H	4.027970	2.292232	-0.062786
H	2.300659	-4.024155	-0.061391
H	-2.300659	4.024155	-0.061391
S	0.000000	0.000000	-7.303239
S	0.000000	0.000000	7.204045

u-$Cr_3(L)_4(NCS)_2$ (0.71)

E = -23.719240 au

Cr	0.000000	0.000000	-2.432318
Cr	0.000000	0.000000	0.207682
Cr	0.000000	0.000000	2.137682
N	-1.458588	-1.399150	-0.015674
N	1.458588	1.399150	-0.015674
N	1.398671	-1.459546	-0.017088
N	-1.398671	1.459546	-0.017088
N	-0.843278	-1.916640	-2.195151
N	0.843278	1.916640	-2.195151
N	1.915909	-0.844822	-2.196737
N	-1.915909	0.844822	-2.196737

N	-1.924062	-0.858069	2.163942
N	1.924062	0.858069	2.163942
N	0.857464	-1.924565	2.162830
N	-0.857464	1.924565	2.162830
N	0.000000	0.000000	4.314926
N	0.000000	0.000000	-4.509145
C	-1.444418	-2.311715	-1.032325
C	1.444418	2.311715	-1.032325
C	2.310338	-1.447628	-1.034585
C	-2.310338	1.447628	-1.034585
C	-2.366153	-1.434621	1.006452
C	2.366153	1.434621	1.006452
C	1.432765	-2.367354	1.004952
C	-1.432765	2.367354	1.004952
C	-1.914646	-3.636947	-0.904672
C	1.914646	3.636947	-0.904672
C	3.633902	-1.922999	-0.908833
C	-3.633902	1.922999	-0.908833
C	-3.690387	-1.906187	0.911980
C	3.690387	1.906187	0.911980
C	1.900653	-3.692854	0.909756
C	-1.900653	3.692854	0.909756
C	-0.729861	-2.796071	-3.214327
C	0.729861	2.796071	-3.214327
C	2.794415	-0.733757	-3.216941
C	-2.794415	0.733757	-3.216941
C	-2.753788	-0.771994	3.222797
C	2.753788	0.771994	3.222797
C	0.769470	-2.754840	3.221173
C	-0.769470	2.754840	3.221173
C	-1.202240	-4.092924	-3.152489
C	1.202240	4.092924	-3.152489
C	4.089404	-1.211604	-3.157154
C	-4.089404	1.211604	-3.157154
C	-4.052496	-1.248303	3.196933
C	4.052496	1.248303	3.196933
C	1.241890	-4.054867	3.194396
C	-1.241890	4.054867	3.194396
C	-1.798141	-4.518549	-1.960055
C	1.798141	4.518549	-1.960055
C	4.514301	-1.809686	-1.965527
C	-4.514301	1.809686	-1.965527
C	-4.526843	-1.814562	2.008424
C	4.526843	1.814562	2.008424
C	1.806246	-4.530105	2.005374
C	-1.806246	4.530105	2.005374
C	0.000000	0.000000	-5.707617
C	0.000000	0.000000	5.512014
H	-0.243824	-2.407921	-4.109221
H	0.243824	2.407921	-4.109221
H	2.406803	-0.245961	-4.111111
H	-2.406803	0.245961	-4.111111
H	-2.328494	-0.300934	4.107534
H	2.328494	0.300934	4.107534

H	0.299731	-2.328837	4.106252
H	-0.299731	2.328837	4.106252
H	-1.091778	-4.753942	-4.011000
H	1.091778	4.753942	-4.011000
H	4.749670	-1.103669	-4.016549
H	-4.749670	1.103669	-4.016549
H	-4.681713	-1.157645	4.081465
H	4.681713	1.157645	4.081465
H	1.149524	-4.684335	4.078588
H	-1.149524	4.684335	4.078588
H	-2.149000	-5.546181	-1.849460
H	2.149000	5.546181	-1.849460
H	5.540632	-2.164873	-1.856600
H	-5.540632	2.164873	-1.856600
H	-5.558655	-2.162456	1.933410
H	5.558655	2.162456	1.933410
H	2.150756	-5.562972	1.929433
H	-2.150756	5.562972	1.929433
H	-2.322913	-3.963538	0.050842
H	2.322913	3.963538	0.050842
H	3.960381	-2.333051	0.045947
H	-3.960381	2.333051	0.045947
H	-4.051982	-2.295142	-0.039151
H	4.051982	2.295142	-0.039151
H	2.288327	-4.054864	-0.041715
H	-2.288327	4.054864	-0.041715
S	0.000000	0.000000	-7.319473
S	0.000000	0.000000	7.127373

Cartesian Coordinates of the scattering region – symmetric $Cr_3(L)_4(SCN)_2$ attached to electrodes with 32 and 48 Au atoms.

Au	0	0	7.06
Au	-1.44	2.5	7.06
Au	-2.88	4.99	7.06
Au	-4.33	7.49	7.06
Au	2.88	0	7.06
Au	1.44	2.5	7.06
Au	0	4.99	7.06
Au	-1.44	7.49	7.06
Au	5.77	0	7.06
Au	4.33	2.5	7.06
Au	2.88	4.99	7.06
Au	1.44	7.49	7.06
Au	8.65	0	7.06
Au	7.21	2.5	7.06
Au	5.77	4.99	7.06
Au	4.33	7.49	7.06
Au	-4.33	9.16	9.42
Au	0	1.66	9.42
Au	-1.44	4.16	9.42

Au	-2.88	6.66	9.42
Au	-1.44	9.16	9.42
Au	2.88	1.66	9.42
Au	1.44	4.16	9.42
Au	0	6.66	9.42
Au	1.44	9.16	9.42
Au	5.77	1.66	9.42
Au	4.33	4.16	9.42
Au	2.88	6.66	9.42
Au	4.33	9.16	9.42
Au	8.65	1.66	9.42
Au	7.21	4.16	9.42
Au	5.77	6.66	9.42
Cr	1.44	5.83	16.27
Cr	1.44	5.83	18.63
Cr	1.44	5.83	20.99
N	2.74	4.26	18.63
N	0.14	7.39	18.63
N	-0.12	4.53	18.63
N	3	7.12	18.63
N	2.12	3.83	16.44
N	0.76	7.82	16.44
N	-0.56	5.15	16.44
N	3.44	6.5	16.44
N	3.27	4.79	20.82
N	-0.39	6.86	20.82
N	0.4	3.99	20.82
N	2.48	7.66	20.82
N	1.44	5.83	23.08
N	1.44	5.83	14.18
C	2.66	3.36	17.61
C	0.22	8.29	17.61
C	-1.03	4.6	17.61
C	3.91	7.05	17.61
C	3.63	4.16	19.65
C	-0.75	7.49	19.65
C	-0.22	3.63	19.65
C	3.1	8.02	19.65
H	2.93	2.31	17.69
H	-0.05	9.35	17.69
H	-2.08	4.34	17.69
H	4.96	7.31	17.69
H	4.62	3.71	19.57
H	-1.74	7.94	19.57
H	-0.68	2.65	19.57
H	3.56	9.01	19.57
H	1.98	3.2	15.67
H	0.9	8.46	15.67
H	-1.19	5.28	15.67
H	4.07	6.37	15.67
H	3.92	4.8	21.59

H	-1.04	6.85	21.59
H	0.41	3.34	21.59
H	2.47	8.31	21.59
C	1.44	5.83	12.98
C	1.44	5.83	24.28
S	1.44	5.83	11.37
S	1.44	5.83	25.89
Au	0	0	27.87
Au	-1.44	2.5	27.87
Au	-2.88	4.99	27.87
Au	-4.33	7.49	27.87
Au	2.88	0	27.87
Au	1.44	2.5	27.87
Au	0	4.99	27.87
Au	-1.44	7.49	27.87
Au	5.77	0	27.87
Au	4.33	2.5	27.87
Au	2.88	4.99	27.87
Au	1.44	7.49	27.87
Au	8.65	0	27.87
Au	7.21	2.5	27.87
Au	5.77	4.99	27.87
Au	4.33	7.49	27.87
Au	-4.33	9.16	30.22
Au	0	1.66	30.22
Au	-1.44	4.16	30.22
Au	-2.88	6.66	30.22
Au	-1.44	9.16	30.22
Au	2.88	1.66	30.22
Au	1.44	4.16	30.22
Au	0	6.66	30.22
Au	1.44	9.16	30.22
Au	5.77	1.66	30.22
Au	4.33	4.16	30.22
Au	2.88	6.66	30.22
Au	4.33	9.16	30.22
Au	8.65	1.66	30.22
Au	7.21	4.16	30.22
Au	5.77	6.66	30.22
Au	-2.88	8.32	32.58
Au	1.44	0.83	32.58
Au	0	3.33	32.58
Au	-1.44	5.83	32.58
Au	0	8.32	32.58
Au	4.33	0.83	32.58
Au	2.88	3.33	32.58
Au	1.44	5.83	32.58
Au	2.88	8.32	32.58
Au	7.21	0.83	32.58
Au	5.77	3.33	32.58
Au	4.33	5.83	32.58

Au	5.77	8.32	32.58
Au	10.09	0.83	32.58
Au	8.65	3.33	32.58
Au	7.21	5.83	32.58